Priority Brief

Cancer Immunology Research

Systemic Interferon-γ Increases MHC Class I Expression and T-cell Infiltration in Cold Tumors: Results of a Phase 0 Clinical Trial

Shihong Zhang[1], Karan Kohli[1], R. Graeme Black[1], Lu Yao[1], Sydney M. Spadinger[1], Qianchuan He[2], Venu G. Pillarisetty[3], Lee D. Cranmer[1,4], Brian A. Van Tine[5], Cassian Yee[6], Robert H. Pierce[1], Stanley R. Riddell[1,4], Robin L. Jones[7], and Seth M. Pollack[1,4]

Abstract

Interferon-γ (IFNγ) has been studied as a cancer treatment with limited evidence of clinical benefit. However, it could play a role in cancer immunotherapy combination treatments. Despite high expression of immunogenic cancer–testis antigens, synovial sarcoma (SS) and myxoid/round cell liposarcoma (MRCL) have a cold tumor microenvironment (TME), with few infiltrating T cells and low expression of major histocompatibility complex class I (MHC-I). We hypothesized that IFNγ treatment could drive inflammation in a cold TME, facilitating further immunotherapy. We conducted a phase 0 clinical trial treating 8 SS or MRCL patients with weekly systemic IFNγ. We performed pre- and posttreatment biopsies. IFNγ changed the SS and MRCL TME, inducing tumor-surface MHC-I expression and significant T-cell infiltration ($P < 0.05$). Gene-expression analysis suggested increased tumor antigen presentation and less exhausted phenotypes of the tumor-infiltrating T cells. Newly emergent antigen-specific humoral and/or T-cell responses were found in 3 of 7 evaluable patients. However, increased expression of PD-L1 was observed on tumor-infiltrating myeloid cells and in some cases tumor cells. These findings suggest that systemic IFNγ used to convert SS and MRCL into "hot" tumors will work in concert with anti–PD-1 therapy to provide patient benefit.

Introduction

Interferon-γ (IFNγ) is an FDA-approved cytokine therapy, used as a standard-of-care treatment for osteopetrosis and chronic granulomatous disease. In the 1990s, IFNγ was evaluated as a single-agent cancer immunotherapy in several prospective randomized trials (1–3). These trials found no benefit in cancer and thus IFNγ was largely written off as an ineffective treatment. However, these studies were done prior to the modern era of immunotherapy. The failure of IFNγ to demonstrate efficacy may have been partly a result of checkpoint upregulation, particularly PD-L1 (4–6).

IFNγ can enhance expression of surface major histocompatibility complex (MHC) molecules and increase the processing and presentation of tumor-specific antigens (7), thus facilitating T-cell recognition and cytotoxicity (8–11). However, even though IFNγ is one of the best-studied cytokines in animal models and has undergone extensive clinical testing, little is known regarding the impact of IFNγ on the immune cells of the human tumor microenvironment (TME). Most of the clinical studies focus on the efficacy of IFNγ, although one study shows increased MHC expression on tumor cells in fine-needle aspirates from melanoma patients treated with IFNγ (12). Interest in IFNγ has resurged as investigators have uncovered possible synergy between IFNγ and PD-1 inhibitors (for example, see clinical trials NCT02614456, NCT03063632 on clinicaltrials.gov). Therefore, understanding the molecular mode of action of IFNγ may be key for cancer immunotherapy development.

Our group has been interested in developing immunotherapy for two immunologically quiet (also called "cold") tumors (13): synovial sarcoma (SS) and myxoid/round cell liposarcoma (MRCL). These malignancies are translocation driven and have a low mutational burden but highly express cancer–testis antigens, e.g., NY-ESO-1, PRAME, and MAGE families (14, 15). Encouraging results have been observed in trials using NY-ESO-1–specific vaccines (16) and TCR-transduced T-cell therapies but the response rate and durability need to be increased (17, 18). One obstacle is that SS and MRCL have low MHC class I (MHC-I) expression (19) and few infiltrating T cells, both of which likely help the tumor evade adoptive T-cell therapy and other immunotherapies. Although a number of injectable agents can inflame the TME in a single tumor site, we hypothesized that systemic, subcutaneous IFNγ could induce widespread

[1]Clinical Research Division, Fred Hutchinson Cancer Research Center, Seattle, Washington. [2]Public Health Sciences Division, Fred Hutchinson Cancer Research Center, Seattle, Washington. [3]Department of Surgery, University of Washington, Seattle, Washington. [4]Division of Medical Oncology, University of Washington, Seattle, Washington. [5]Division of Oncology, Washington University in St. Louis, St. Louis, Missouri. [6]Department of Melanoma Medical Oncology, The University of Texas MD Anderson Cancer Center, Houston, Texas. [7]Sarcoma Unit, Royal Marsden Hospital and Institute of Cancer Research, London, UK.

Note: Supplementary data for this article are available at Cancer Immunology Research Online (http://cancerimmunolres.aacrjournals.org/).

Corresponding Author: Seth M. Pollack, Fred Hutchinson Cancer Research Center, 1100 Fairview Ave N, D3-100, Seattle, WA 98109. Phone: 206-667-6629; E-mail: spollack@fredhutch.org

Cancer Immunol Res 2019;7:1237–43

doi: 10.1158/2326-6066.CIR-18-0940

tumor inflammation potentially allowing for more effective immunotherapy combinations. Here we describe results of a pilot phase 0 trial, with the primary objective of determining whether systemic weekly subcutaneous IFNγ treatment would increase MHC-I expression in SS and MRCL patients.

Materials and Methods

Clinical protocol and sample collection

Informed written consent in accordance with the Declaration of Helsinki was obtained from all subjects prior to enrollment in an IRB-approved protocol (NCT01957709); eligibility criteria are listed in Supplementary Table S1. Patients generally received 4 weekly injections of IFNγ 100 μg/m^2; however, to accommodate patient schedules as few as 2 injections were allowed. Core needle biopsies were performed prior to starting IFNγ and 1 to 3 days after their last dose. Toxicity data were tabulated using CTCAE v4.0. The primary objective was to determine whether IFNγ would increase MHC-I expression. Secondary objectives were to determine whether IFNγ increased MHC-II expression and to examine the changes seen in the immune infiltrates of SS and MRCL tumors.

Patient sample preparation and flow cytometry

Core needle biopsy specimens were either formalin-fixed paraffin-embedded (FFPE) or placed in RPMI-1640 media for other studies. To prepare single-cell suspensions, tumor specimens were cut into 1 to 2 mm fragments, incubated in an enzymatic cocktail containing Type IV collagenase, DNase, and hyaluronidase for 30 minutes at 37°C, then pressed through a 70-μm mesh cell strainer. Flow cytometry was performed on the same day as biopsy collection using a multicolor panel. Detailed staining panel is listed in Supplementary Table S2. Stained samples were analyzed on a BD FACSAria II. CD45$^-$ tumor cells, CD8$^+$ T cells, and CD4$^+$ T cells were sorted separately from live single cells. HLA-ABC and PD-L1 gates made on the tumor cells were determined by T-cell gates as positive and negative controls, respectively. Statistical comparison of pre- and posttreatment flow cytometry was performed using two-sided Wilcoxon signed-rank test.

Serum cytokine measurement

Serum samples were collected and stored at −20°C. Pre- and posttreatment paired serum samples from the same patient were thawed and analyzed at the same time using the following kits from Thermo Fisher: Immune Monitoring 65-Plex Human ProcartaPlex Panel and Immuno-Oncology Checkpoint 14-Plex Human ProcartaPlex Panel 1. Samples were measured in duplicate, following the manufacturer's protocol.

Gene-expression profiling

RNA from tumor cells and tumor-infiltrating CD8$^+$ T cells from patients #6, #7, and #8 (the last 3 patients on study) were extracted individually using Qiagen AllPrep DNA/RNA Micro Kit. Gene-expression profiling was performed by the Affymetrix Clariom D Pico assay platform. Microarray data were then normalized and analyzed by limma. Gene set enrichment analysis (GSEA) was performed with preranked lists using the GSEA software (20). $\log_2$ fold change preranked lists were generated with posttreatment $\log_2$ value subtracted by pretreatment $\log_2$ value generated by limma. Tests were run with the preranked lists from each individual and gene sets of interest with 1,000 permutations.

PBMC *in vitro* stimulation and intracellular cytokine staining (ICS)

Cryopreserved patients' PBMCs from the same patients of different time points were thawed and cultured at the same time. PBMCs were cultured for 10 days in STEMCELL-XF T-cell expansion medium with 50 IU/mL of IL2, in the presence of 15-mer, overlapping by 11 amino acid peptide pools derived from human NY-ESO-1, MAGE-A4, or PRAME proteins (JPT), or without peptide as a negative control. Half medium change was performed every 3 to 4 days. On day 10, cells were restimulated with the same stimulant as in culture for 6 hours, with the presence of brefeldin A (eBioscience) for the last 5 hours. Single peptide concentrations used in culture and restimulation were both 1 μg/mL. Staining of CD4-BV421, CD8-APC-Cy7, and eBioscience fixable viability dye eFluor 506 was performed prior to permeabilization and fixation using the BD Fixation/Permeabilization Solution Kit. IFNγ-FITC and TNFPE-Cy7 were stained intracellularly for 30 minutes prior to flow cytometry analysis.

Serum tumor antigen–specific antibody measurement

Serum antibodies specific for tumor antigens were measured by Serametrix. The detailed antigen list is shown in Supplementary Fig. S1. Highly positive responses shown in the Results are defined as >9-fold over background, and the background is lower quartile of all serum data after Gnjatic and colleagues (21). Because antibodies usually take about 4 weeks to be detected after the host is exposed to a certain antigen, we only tested sera when it was available at least 4 weeks posttreatment for this analysis.

Multiplex immunohistochemistry (mIHC) sample processing and staining procedure

Staining was performed on 4-μm thick FFPE sections by using automated staining. After deparaffinization, slides were treated with antigen retrieval (AR) buffer (Diva Decloaker from BioCare Medical or Leica Bond Epitope Retrieval Solution 2) and heated for 15 minutes at 95 to 100°C. Slides were allowed to cool in the AR buffer for 15 minutes at room temperature and were then rinsed with deionized water and 1 × Tris-buffered saline with Tween-20. Endogenous peroxidase was blocked using 3% hydrogen peroxide. Protein stabilization and background reduction was done using intelliPATH Background Punisher. Slides were then incubated for 1 hour with primary antibodies against HLA-ABC (clone EMR8-5), PD-L1 (clone RBT-PDL1) followed by the secondary antibody (PerkinElmer OPAL Polymber HRP Ms Plus Rb) application for 30 minutes and the application of the tertiary TSA-amplification reagent (PerkinElmer OPAL fluor) for 10 minutes. Antigen stripping was performed either by heating with Leica Bond Epitope Retrieval Solution 2 or with Biocare medical denaturation reagent at room temperature. Slides were imaged with either Leica Aperio FL Immunofluorescence slide scanner or Leica SP8 confocal microscope.

Results

Patient demographics and clinical data

Eight patients (mean age 51, range, 24–68) were treated with 2 to 4 doses of IFNγ weekly 100 μg/m^2. Patients' information is listed in Table 1. Seven were evaluable for both pre- and post-treatment biopsy samples; patient # 3 refused to undergo a posttreatment biopsy. Six patients had SS and two had MRCL. Two patients received less than the full 4-week course in order to

Table 1. Patient information and treatment history

ID	Subtype	Sex	Age	Treatment duration	Prior treatment
1	MRCL	M	68	4 weeks	Surgery, radiation, chemo, LV305
2	SS	F	60	2 weeks	(Refused chemotherapy)
3	SS	M	50	4 weeks	Chemo, LV305
4	SS	M	67	4 weeks	Surgery, chemo, radiation
5	MRCL	M	49	4 weeks	Surgery, chemo, radiation, LV305
6	SS	F	38	3 weeks	Radiation, surgery, LV305, atezolizumab
7	SS	M	54	4 weeks	Surgery, radiation, chemo
8	SS	F	24	4 weeks	Radiation, surgery, chemo

NOTE: LV305 is an NY-ESO-1 vaccine that patients received as part of a clinical trial. Some patients received monoclonal antibody treatments as part of their chemotherapy, including olaratumab (anti-PDGFRα), or on a clinical trial of MorAb-004 (anti-endosialin).

accommodate their schedules, as was permitted on this phase 0 trial. Following his treatment, on examination of ultrasound studies, it was found that patient #7 had his pretreatment biopsy taken very close to an area that had been radiated several weeks prior, where acute radiation-related inflammation was likely occurring. Although data from this patient were not censured, this was considered during data interpretation as their results differed from other patients. No patients had unexpected grade 3 or higher toxicity due to treatment and none discontinued treatment due to toxicity. All toxicity resolved completely or to grade 1 by 72 hours after injection. A list of all adverse events can be found in Supplementary Table S3.

Tumor cell antigen processing and presentation

Tumor single-cell suspension from both pre- and posttreatment time points were prepared and analyzed for surface MHC-I and -II molecules from all 7 evaluable patients. Overall, the percentage of MHC-I$^+$ cells in the CD45$^-$ fraction was increased in posttreatment samples (1.39%–92.2%, median 26.6%) compared with pretreatment (0.131%–51.6%, median 8.91%). Major (>30%) and moderate (15%–30%) increases in MHC-I$^+$ were observed in 4 out 7 patients (#2, #4, #6, and #8). Although patients #1 and #5 had only minor increases in HLA-ABC (<15% increase), their tumor cells were negative for HLA-ABC pretreatment, and HLA-ABC$^+$ populations became detectable posttreatment (Fig. 1A and B), suggesting that although the increases were small in magnitude they may be clinically relevant. Patient #7, whose pretreatment biopsy may have been influenced by receipt of radiotherapy shortly before biopsy, was the only patient in whom HLA-ABC decreased posttreatment. The intensity of HLA-ABC expression also increased by mIHC in patients with available FFPE samples (Fig. 1C). These data suggest that tumor cells express HLA-ABC more abundantly and intensely after IFNγ treatment. In contrast, the MHC-II molecule HLA-DR did not change significantly on SS or MRCL tumor cells.

Gene-expression profiling was performed on sorted tumor cells from the biopsy samples of patients #6, #7, and #8. GSEA, with the KEGG antigen processing and presentation gene set, was adopted for this assessment. GSEA results were consistent with

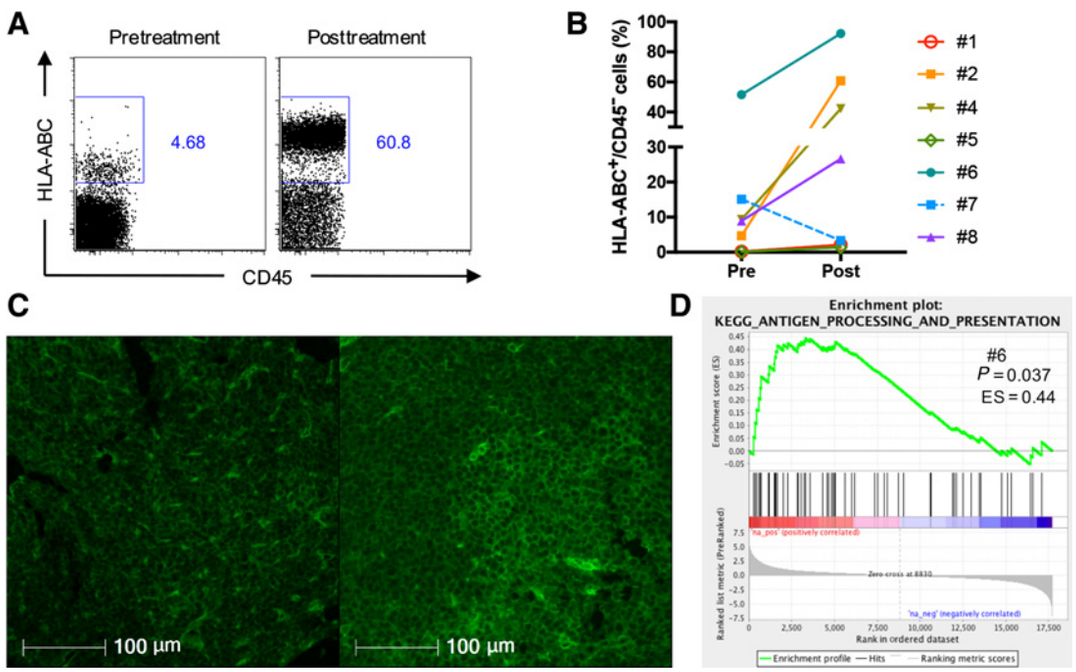

Figure 1.
Increase of tumor-surface HLA-ABC, tumor antigen presentation after IFNγ treatment in SS and MRCL patients. **A,** Representative flow plots of HLA-ABC molecule expression on pretreatment (left) and posttreatment (right) CD45$^-$ tumor cells from patient #2. **B,** HLA-ABC expression change from all patients analyzed. Patient #7, who had pretreatment radiation, is an outlier and thus labeled with dotted line ($P = 0.037$, excluding outlier, statistical analysis was performed with Wilcoxon signed-rank test.). **C,** IHC staining of tumor tissue slides from patient #2 pre- (left) and posttreatment (right) biopsies. Green fluorophore stains HLA-ABC. In both pre- and post-images, cells located at the vascular-like structure express a high density of HLA-ABC. These cells are presumably endothelial cells and can therefore serve as internal controls for HLA-ABC expression change in tumor cells. **D,** GSEA using KEGG antigen processing and presentation gene set. The preranked list was generated with $\log_2$-fold change of gene expression from tumor cells, and the analysis was done with the GSEA software by Broad Institute. The result shows increased antigen processing and presentation of tumor cells from patient #6.

the tumor-surface HLA-ABC expression. Patient #6, who had a 41% increase of tumor-surface HLA-ABC expression, also had significantly higher antigen processing and presentation capability after treatment, whereas little change was observed in patient #8 who had moderate increase in HLA-ABC (17%) and patient #7 had decreased antigen processing and presentation (Fig. 1D; Supplementary Fig. S2). This effect was also seen in other genes related to antigen presentation; $\log_2$ expression of *TAP1* in patient #6 pretreatment increased from 3.77 to 6.87. Gene-expression profiling confirmed expression of commonly found tumor antigens (Supplementary Fig. S3). The major responder patient #6 also had a more apoptotic tumor gene-expression profile (Supplementary Fig. S4), suggesting the possibility of immune-mediated tumor cell apoptosis.

Change in T-cell infiltration and phenotype

Pretreatment, low frequencies of tumor-infiltrating T cells (% $CD45^+CD3^+$ in live cells from single-cell suspensions) were observed. All but one patient had fewer than 0.5% of their pretreatment tumor comprised of T cells (0.015%–1.05%, median 0.14%). T-cell percentages increased by >0.5% in 5 patients posttreatment, with a max of 3.39% (0.074%–3.39%, median 0.82%; $P = 0.03$; Fig. 2A). Except for patient #1, all subjects had $CD8^+$ T-cell biased infiltration, and IFNγ did not change the dominance of $CD8^+$ or $CD4^+$ T-cell infiltrates (Supplementary Fig. S5). T-cell infiltration was correlated with the tumor-surface HLA-ABC expression in our cohort ($r^2 = 0.59$, $P = 0.001$; Fig. 2B), suggesting the increase of T-cell infiltration may have been driven by the tumor HLA-ABC expression.

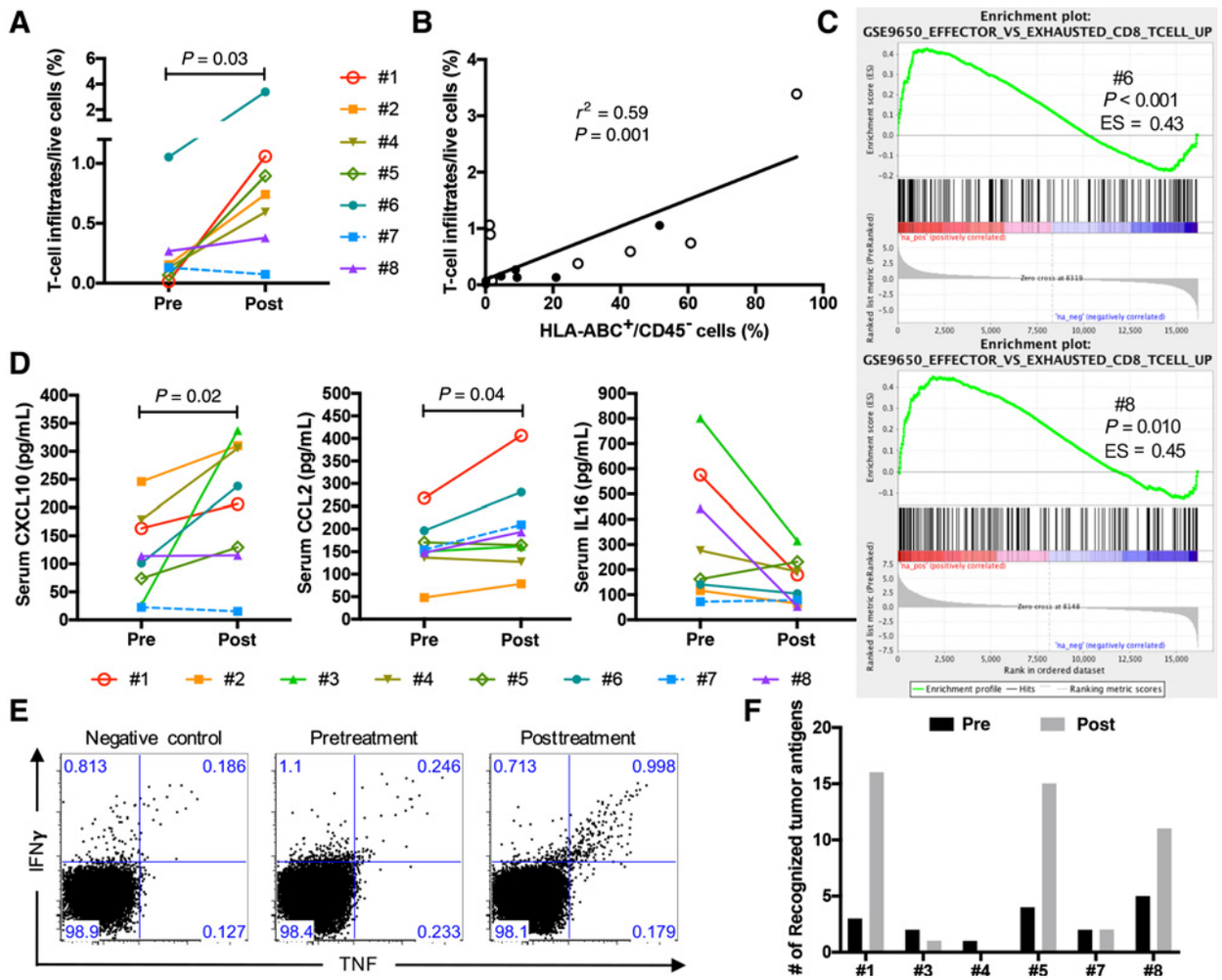

Figure 2.

Increase of T-cell infiltration and functionality after IFNγ treatment. **A,** Percentages of $CD45^+CD3^+$ cells out of all live cells from the analyzed tumor single-cell suspension from all 7 patients tested. T cells significantly increased ($P = 0.03$). Statistical analysis was performed with Wilcoxon signed-rank test. **B,** Correlation of T-cell infiltration and tumor-surface HLA-ABC expression. Closed and open dots represent samples from pretreatment and posttreatment, respectively. **C,** GSEA analysis of patients #6 and #8 $CD8^+$ TIL reveals a more effector phenotype after treatment, comparing with a more exhausted phenotype before treatment. **D,** Individual plots of serum CXCL10, CCL2, and IL16 concentrations. **E,** ICS shows patient #1 had an increased NY-ESO-1–specific T-cell response posttreatment (right) compared with pretreatment (middle). These plots were gated on $CD4^+$ single live cells and are representative of results from 3 independent experiments done on different PBMC aliquots from the same samples. **F,** Numbers of tumor antigens that are recognized by serum antibodies in 6 patients who received IFNγ treatment for 4 weeks.

Gene-expression profiling of $CD8^+$ TIL phenotypes was available from patients #6 and #8. GSEA analysis using previously defined gene sets (22) revealed that in both subjects, pretreatment $CD8^+$ TIL exhibited an exhausted phenotype and demonstrated a significant conversion toward an effector phenotype after IFNγ treatment ($P < 0.001$ for patient #6; $P < 0.01$ for patient #8, Fig. 2C). These results suggest that IFNγ treatment either reversed TIL exhausted state or, more likely, induced infiltration of nonexhausted T cells.

Serum cytokine change

A total of 79 cytokines, chemokines, and other molecules were measured in sera (Supplementary Fig. S6). CXCL10, also known as interferon-inducible protein 10 (IP10), was significantly increased among all patients, demonstrating the systemic response from subcutaneous injections (Fig. 2D). For individuals, CXCL10 concentration changes were consistent with the tumor-surface HLA-ABC expression and antigen presentation changes. In addition, increased CCL2 and decreased IL16 expression was observed after treatment, which, like CXCL10, have chemoattractant roles and may be related to immune cell migration and infiltration into the tumors.

Induction of tumor-specific immune responses

We next compared antigen-specific T cells for NY-ESO-1, MAGE-A4, and PRAME in peripheral blood (Supplementary Fig. S3). T-cell responses to cancer–testis antigens are difficult to detect in the blood of SS and MRCL patients without extensive culture and stimulation (23). Nevertheless, NY-ESO-1–specific T-cell responses developed following IFNγ treatment in patient #1 (Fig. 2E). Before treatment, as indicated by ICS, no NY-ESO-1–specific response was detectable from patient #1. After treatment, an $IFN\gamma^+TNF\alpha^+CD4^+$ T-cell population was seen upon NY-ESO-1 peptide pool stimulation. Patient #1 had predominantly $CD4^+$ T-cell infiltration, suggesting that $CD4^+$ T-cell help may be important for immunity against SS. Serum antibodies specific to 29 tumor antigens were measured from the pre- and posttreatment sera. Three patients (#1, #5, and #8) developed humoral responses against more tumor antigens following treatment, with an average of 4 (pre-) antigen specificities increasing to 14 (posttreatment; Supplementary Fig. S1, and Fig. 2F).

Increase of tumor and myeloid cell PD-L1 expression

We next evaluated PD-L1 expression on both tumor cells and tumor-infiltrating myeloid cells. Based on flow cytometry, 2 out of the 7 patients had increases of $PD\text{-}L1^+$ tumor cell percentages. Before treatment, both patients #2 and #8 had <5% $PD\text{-}L1^+$ tumor cells, whereas after treatment, $PD\text{-}L1^+$ increased to 64% and 15%, respectively (Fig. 3A and B). An increased percentage of $PD\text{-}L1^+$ cells was found on posttreatment tumor-infiltrating myeloid cells in all patients analyzed. Compared with pretreatment (0.694%–97.1%, median 34.6%), $PD\text{-}L1^+$ myeloid cell numbers increased significantly after IFNγ treatment (33.6%–100%, median 55.8%. $P = 0.03$; Fig. 3C and D). This increased PD-L1 expression on tumor cells and myeloid cells in the tumor may function to regulate the newly activated T cells in the TME.

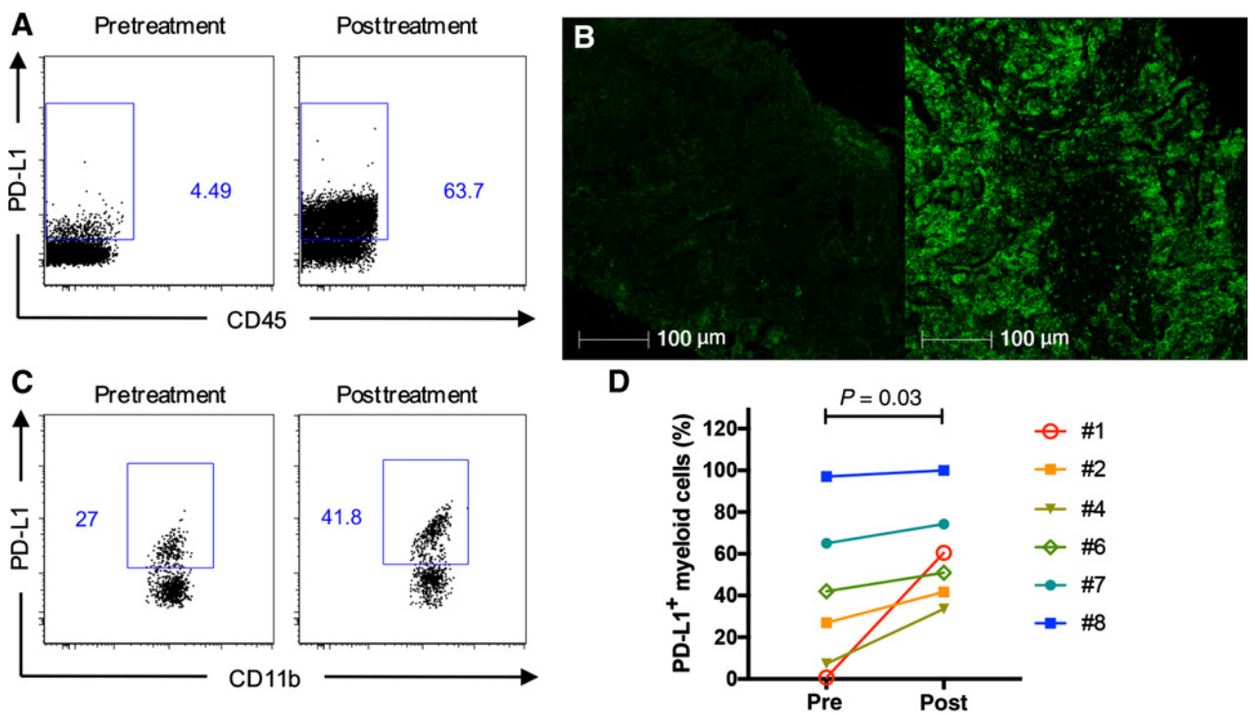

Figure 3.

PD-L1 expression increased on tumor cells and tumor-infiltrating myeloid cells after IFNγ treatment. **A,** Pre- and posttreatment flow plots of PD-L1 expression on $CD45^-$ tumor cells from patient #2 tumor biopsies. **B,** IHC images showing PD-L1 expression increase on patient #4 tumor biopsies. **C,** Pre- and posttreatment flow plots of PD-L1 expression on $CD11b^+$ myeloid cells from patient #2 tumor biopsies. **D,** $PD\text{-}L1^+$ myeloid cells increase following treatment ($P = 0.03$). Statistical analysis was performed with Wilcoxon signed-rank test.

Discussion

In this report, we present the results of a phase 0 trial using weekly IFNγ in patients with SS and MRCL. Although the analysis of these patients was limited by a small sample size, we did observe that, although SS and MRCL have cold TMEs, expression of HLA-ABC and T-cell infiltration can increase after IFNγ treatment. IFNγ is used in two FDA-approved indications and multiple large randomized studies. We provide here detailed analyses of the impact of IFNγ on human tumors focusing on the effect of IFNγ on the TME of cold solid tumors that generally have a low mutation burden.

Although PD-L1 is an imperfect biomarker, its expression has been correlated with response to PD-1 blockade. IFNγ can induce tumor PD-L1 expression in laboratory models of different cancer types, including melanoma, gastric, and ovarian cancers (4–6). Here we show this induction clinically, in two tumors (SS and MRCL) that generally lack strong PD-L1 expression in the untreated setting (19). PD-L1 is consistently upregulated on tumor-infiltrating myeloid cells in response to inflammation, which may also suppress T-cell functions and is more important than PD-L1 expression on tumor cells in some models (24, 25). We also analyzed other potential immune-escape mechanisms followed by IFNγ treatment, including impairment of IFNγ pathway and upregulation of other immune inhibitory molecules. We saw no significant changes, possibly due to the small number of patients, but these theoretical mechanisms should be kept in mind in future studies.

In summary, our results demonstrate that the cold TME of SS and MRCL was malleable and could be altered to facilitate immunotherapy. Based on these data, a cohort of patients is being added to the multicenter Cancer Immunotherapy Networks (CITN) trial CITN-13 (NCT03063632) to test combining IFNγ with pembrolizumab for SS patients.

Disclosure of Potential Conflicts of Interest

V.G. Pillarisetty reports receiving a commercial research grant from Merck and is a consultant/advisory board member for the same. L.D. Cranmer reports receiving a commercial research grant from Eli Lilly, Tracon, AADi, and Exelixis and is a consultant/advisory board member for Blueprint and Regeneron. B.A. Van Tine reports receiving a commercial research grant from Merck, Pfizer, and Tracon, has received honoraria from the speakers bureau of Caris, Janseen, and Lilly, is a consultant/advisory board member for Epizyme, Lilly, CytRX, Janssen, Immune Design, Daiichi Sankyo, Plexxicon, and Adaptimmune, and has received an expert testimony from Lilly. C. Yee has ownership interest (including stock, patents, etc.) in Immatics US, is a consultant/advisory board member for Immatics US and Berkeley Lights. S. Riddell reports receiving a commercial research grant from, has ownership interest (including stock, patents, etc.) in, and is a consultant/advisory board member for Juno Therapeutics, a Celgene company. R.L. Jones is a consultant/advisory board member for Adaptimmune, Blueprint, Pharmamr, Tracon, Clinigen, Eisai, Epizyme, Daichii, Deciphera, Immundesign, Lilly, and Merck. S.M. Pollack reports having received honoraria from Seattle Genetics, Bayer, Tempus, Daiichi Sankyo, Blueprint and grants and research funding from Merck, EMD Sereno, Incyte, Presage, Janssen, Oncosec, Juno Therapeutics. No potential conflicts of interest were disclosed by the other authors.

Authors' Contributions

Conception and design: S. Zhang, C. Yee, R.L. Jones, S.M. Pollack
Development of methodology: S. Zhang, K. Kohli, C. Yee, R.H. Pierce, R.L. Jones, S.M. Pollack
Acquisition of data (provided animals, acquired and managed patients, provided facilities, etc.): K. Kohli, R.G. Black, S.M. Spadinger, L.D. Cranmer, B.A. Van Tine, R.H. Pierce, R.L. Jones, S.M. Pollack
Analysis and interpretation of data (e.g., statistical analysis, biostatistics, computational analysis): S. Zhang, K. Kohli, L. Yao, L.D. Cranmer, B.A. Van Tine, R.H. Pierce, R.L. Jones, S.M. Pollack
Writing, review, and/or revision of the manuscript: S. Zhang, K. Kohli, R.G. Black, S.M. Spadinger, Q. He, V.G. Pillarisetty, L.D. Cranmer, B.A. Van Tine, S. Riddell, R.L. Jones, S.M. Pollack
Administrative, technical, or material support (i.e., reporting or organizing data, constructing databases): S. Zhang, R.L. Jones
Study supervision: B.A. Van Tine, R.L. Jones, S.M. Pollack

Acknowledgments

Interferon-γ was provided for the study by Horizon Pharmaceutical. Support for the trial was also provided by The Gilman Sarcoma Foundation and NIH-NCI K23CA175167.

Received January 3, 2019; revised March 9, 2019; accepted June 3, 2019; published first June 6, 2019.

References

1. Giannopoulos A, Constantinides C, Fokaeas E, Stravodimos C, Giannopoulou M, Kyroudi A, et al. The immunomodulating effect of interferon-gamma intravesical instillations in preventing bladder cancer recurrence. Clin Cancer Res 2003;9:5550–8.
2. Windbichler GH, Constantinides C, Fokaeas E, Stravodimos C, Giannopoulou M, Kyroudi A, et al. Interferon-gamma in the first-line therapy of ovarian cancer: a randomized phase III trial. Br J Cancer 2000; 82:1138–44.
3. Alberts DS, Marth C, Alvarez RD, Johnson G, Bidzinski M, Kardatzke DR, et al. Randomized phase 3 trial of interferon gamma-1b plus standard carboplatin/paclitaxel versus carboplatin/paclitaxel alone for first-line treatment of advanced ovarian and primary peritoneal carcinomas: results from a prospectively designed analysis of progression-free survival. Gynecol Oncol 2008;109:174–81.
4. Garcia-Diaz A, Shin DS, Moreno BH, Saco J, Escuin-Ordinas H, Rodriguez GA, et al. Interferon receptor signaling pathways regulating PD-L1 and PD-L2 expression. Cell Rep 2017;19:1189–201.
5. Mimura K, Teh JL, Okayama H, Shiraishi K, Kua LF, Koh V, et al. PD-L1 expression is mainly regulated by interferon gamma associated with JAK-STAT pathway in gastric cancer. Cancer Sci 2018;109:43–53.
6. Abiko K, Matsumura N, Hamanishi J, Horikawa N, Murakami R, Yamaguchi K, et al. IFN-gamma from lymphocytes induces PD-L1 expression and promotes progression of ovarian cancer. Br J Cancer 2015;112: 1501–9.
7. Shankaran V, Ikeda H, Bruce AT, White JM, Swanson PE, Old LJ, et al. IFNgamma and lymphocytes prevent primary tumour development and shape tumour immunogenicity. Nature 2001;410:1107–11.
8. Gao J, Shi LZ, Zhao H, Chen J, Xiong L, He Q, et al. Loss of IFN-gamma pathway genes in tumor cells as a mechanism of resistance to anti-CTLA-4 therapy. Cell 2016;167:397–404.
9. Ayers M, Lunceford J, Nebozhyn M, Murphy E, Loboda A, Kaufman DR, et al. IFN-gamma-related mRNA profile predicts clinical response to PD-1 blockade. J Clin Invest 2017;127:2930–40.
10. Patel SJ, Sanjana NE, Kishton RJ, Eidizadeh A, Vodnala SK, Cam M, et al. Identification of essential genes for cancer immunotherapy. Nature 2017; 548:537–42.
11. Manguso RT, Pope HW, Zimmer MD, Brown FD, Yates KB, Miller BC, et al. In vivo CRISPR screening identifies Ptpn2 as a cancer immunotherapy target. Nature 2017;547:413–8.
12. Propper DJ, Chao D, Braybrooke JP, Bahl P, Thavasu P, Balkwill F, et al. Low-dose IFN-gamma induces tumor MHC expression in metastatic malignant melanoma. Clin Cancer Res 2003;9:84–92.
13. Thorsson V, Gibbs DL, Brown SD, Wolf D, Bortone DS, Ou Yang TH, et al. The immune landscape of cancer. Immunity 2018;48:812–30.

14. Jungbluth AA, Antonescu CR, Busam KJ, Iversen K, Kolb D, Coplan K, et al. Monophasic and biphasic synovial sarcomas abundantly express cancer/testis antigen NY-ESO-1 but not MAGE-A1 or CT7. Int J Cancer 2001;94:252–6.
15. Pollack SM, Jungbluth AA, Hoch BL, Farrar EA, Bleakley M, Schneider DJ, et al. NY-ESO-1 is a ubiquitous immunotherapeutic target antigen for patients with myxoid/round cell liposarcoma. Cancer 2012;118:4564–70.
16. Pollack SM, Lu H, Gnjatic S, Somaiah N, O'Malley RB, Jones RL, et al. First-in-human treatment with a dendritic cell-targeting lentiviral vector-expressing NY-ESO-1, LV305, induces deep, durable response in refractory metastatic synovial sarcoma patient. J Immunother 2017;40:302–6.
17. Robbins PF, Kassim SH, Tran TL, Crystal JS, Morgan RA, Feldman SA, et al. A pilot trial using lymphocytes genetically engineered with an NY-ESO-1-reactive T-cell receptor: long-term follow-up and correlates with response. Clin Cancer Res 2015;21:1019–27.
18. D'Angelo SP, Melchiori L, Merchant MS, Bernstein D, Glod J, Kaplan R, et al. Antitumor activity associated with prolonged persistence of adoptively transferred NY-ESO-1 (c259)T cells in synovial sarcoma. Cancer Discov 2018;8:944–57.
19. Pollack SM, He Q, Yearley JH, Emerson R, Vignali M, Zhang Y, et al. T-cell infiltration and clonality correlate with programmed cell death protein 1 and programmed death-ligand 1 expression in patients with soft tissue sarcomas. Cancer 2017;123:3291–304.
20. Subramanian A, Tamayo P, Mootha VK, Mukherjee S, Ebert BL, Gillette MA, et al. Gene set enrichment analysis: a knowledge-based approach for interpreting genome-wide expression profiles. Proc Natl Acad Sci U S A 2005;102:15545–50.
21. Gnjatic S, Wheeler C, Ebner M, Ritter E, Murray A, Altorki NK, et al. Seromic analysis of antibody responses in non-small cell lung cancer patients and healthy donors using conformational protein arrays. J Immunol Methods 2009;341:50–8.
22. Wherry EJ, Ha SJ, Kaech SM, Haining WN, Sarkar S, Kalia V, et al. Molecular signature of CD8+ T cell exhaustion during chronic viral infection. Immunity 2007;27:670–84.
23. Pollack SM, Jones RL, Farrar EA, Lai IP, Lee SM, Cao J, et al. Tetramer guided, cell sorter assisted production of clinical grade autologous NY-ESO-1 specific CD8(+) T cells. J Immunother Cancer 2014;2:36.
24. Lau J, Cheung J, Navarro A, Lianoglou S, Haley B, Totpal K, et al. Tumour and host cell PD-L1 is required to mediate suppression of anti-tumour immunity in mice. Nat Commun 2017;8:14572.
25. Tang H, Liang Y, Anders RA, Taube JM, Qiu X, Mulgaonkar A, et al. PD-L1 on host cells is essential for PD-L1 blockade-mediated tumor regression. J Clin Invest 2018;128:580–8.